Proceedings of the
International Conference on Mechanical Engineering and Renewable Energy 2019
(ICMERE2019) 11 – 13 December, 2019, Chittagong, Bangladesh

ICMERE2019-PI-211

CFD ANALYSIS OF VERTICAL KAPLAN TURBINE FOR LOW HEAD AND HIGH FLOW RATE OF WATER

Md. Masbah-Ul-Hakim[1*], **Md. Fahim Faisal**[1]

[1]Department of Mechanical Engineering,
Khulna University of Engineering & Technology,
Khulna-9203, Bangladesh

Email - masbah.067@gmail.com, fahimfaisal081@gmail.com

Abstract*-This paper represents the hydrodynamic analysis of Kaplan turbine using ANSYS CFX. A geometry was generated for runner wheel, spiral volute case and radial guide vanes using Solidworks and Bladegen. Numerical simulations were conducted with no slip condition using transient time step taking inlet velocity as 7.643 m/s. Pressure and velocity distribution at different time steps along the turbine runner blade were observed. Velocity streamline across the rotor blade as well as turbine casing were also investigated. Results showed that the pressure changes gradually from 70898.85 Pa to 20166.90 Pa with the distance increasing from inlet to outlet. On the other hand, velocity decreased sharply from 16.64 m/s to 8.43m/s. Variation of streamwise blade loading was also graphically represented in this paper.*

Keywords: Low Head, Kaplan Turbine, Rotor Blade, CFD, High Flow Rate

1. INTRODUCTION

Hydro, solar, wind, geothermal, wave and tidal current are the major renewable sources available in nature which are known as green alternatives of fossil fuels. Among them, hydropower is the most efficient, reliable source of energy generation. Hydropower or water power is that power derived from the energy of falling water or quick running water, which can be controlled for helpful purposes [1]. Using that power a turbine extracts energy and converts it into useful mechanical work. A turbine may be a turbomachine with a minimum of one moving half referred to as a rotor assembly, which is a shaft or drum with blades attached. Moving fluid acts on the blades so they move and impart motility energy to the rotor. Gas, steam, and water turbines have a casing around the blades that contains and controls the working fluid.

The Kaplan turbine is a propeller-type water turbine that has adjustable blades. It was developed in 1913 by Austrian researcher Viktor Kaplan, combined mechanically adjusted propeller blades with mechanically adjusted wicket gates to attain potency over a good variation of flow and water level. Kaplan turbines are used for low head, only a few meters up to around 30m [2]. The study of hydrodynamics of Kaplan turbine is mainly carried out on the turbine runner. The purpose of a spiral case and guide vanes is to develop a flow field at turbine runner inlet. Hydrodynamic analysis of kaplan turbine is going on from a long time since it gives most efficient power production facility. Several numerical investigations have been done to understand the characteristics of Kaplan turbine. Williamson et al. found that fixed geometry Kaplan turbine is the most effective design option for low head hydropower [3]. Jose et al. [4] performed numerical analysis on runner blades to enhance their performance beyond traditional design. Fluid flow behavior over the blades has been investigated by Chamil Abeykoon [5]. He used different number of blades and shape of blades to optimize the efficiency of the runner wheel. Amiri et al. [6] developed a design of lightweight, low head Kaplan turbine which increased the turbine efficiency by reducing weight, shape alterations, blade angle with combination of materials aluminum alloy, structural steel, titanium alloy as well as stainless steel. In their research, the found that the maximum shear stress developed at the runner blade are maximum at the joints between the hub and runner blade. Charania et al. [7] studied a vertical Kaplan turbine for single phase containing only water for steady state condition. The turbine performance was analyzed at BEP and part load points using CFD. Their investigation was quite satisfactory for BEP and part load conditions. An investigation of the 3D, inviscid, incompressible and steady flow in Kaplan turbine spiral case and distributor was carried out by Muntean et al. [8]. They found that swirling flow formulae perfectly match the numerical data from the 3D flow simulation. A contrast between numerical simulations and measurements of Kaplan turbine is analyzed by Dragica et al. [9]. In their analysis, they used different turbulent models to simulate the steady state conditions. They found that SAS SST and ZLES models are more accurate compared to other models and the discrepancy was between 1%. Motycak et al. [10] observed the conditions of Kaplan turbine

using CFD analysis. They discussed the setting of model, size of the grid and interface definition among the turbine runner and draft.

Since Kaplan turbine is a type of turbomachinery device widely used throughout the world for electric power generation, performance test of Kaplan turbine before manufacturing is a very effective way to reduce cost and time. All the previous works on the Kaplan turbine were either theoretical or experimental. Very few CFD analysis are available on Kaplan turbine and most of them are on runner blade optimization. CFD analysis of Kaplan turbine has been carried out in this paper to investigate the characteristics of vertical Kaplan turbine as well as observe various phenomena such as velocity and pressure distribution using ANSYS as CFD tool.

2. Numerical Methodology

The simulations were conducted using commercially available software package ANSYS CFX V16.0. Several equations had been solved in order to conduct the whole simulations. The general momentum equation is also called the equation of motion or the Navier-Stoke's equation, in addition, the equation of continuity is developed simply by applying the law of conservation of mass to a small volume element within a flowing fluid. The governing continuity and momentum equations are-
Continuity:

$$\frac{\partial \rho}{\partial t} + \frac{\partial}{\partial x}(\rho u) + \frac{\partial}{\partial y}(\rho v) = 0 \quad (1)$$

x momentum:

$$\rho\left(\frac{\partial u}{\partial t} + u\frac{\partial u}{\partial x} + v\frac{\partial u}{\partial y}\right) = \rho g_x - \frac{\partial P}{\partial x} + \mu\left(\frac{\partial^2 u}{\partial x^2} - \frac{\partial^2 u}{\partial y^2}\right) \quad (2)$$

y momentum:

$$\rho\left(\frac{\partial v}{\partial t} + u\frac{\partial u}{\partial x} + v\frac{\partial u}{\partial y} + w\frac{\partial w}{\partial y}\right) = -\frac{\partial P}{\partial x} + \mu\left(\frac{\partial^2 v}{\partial x^2} + \frac{\partial^2 v}{\partial y^2} + \frac{\partial^2 v}{\partial z^2}\right) + \rho g_y \quad (3)$$

z momentum:

$$\rho\left(\frac{\partial w}{\partial t} + u\frac{\partial u}{\partial x} + v\frac{\partial u}{\partial y} + w\frac{\partial w}{\partial y}\right) = -\frac{\partial P}{\partial x} + \mu\left(\frac{\partial^2 w}{\partial x^2} + \frac{\partial^2 w}{\partial y^2} + \frac{\partial^2 w}{\partial z^2}\right) + \rho g_z \quad (4)$$

Here the term -ρg on the right side of the momentum equation represents the body force exerted on the fluid element in the negative x direction.

In order to cope with the turbulent flow conditions, k-ε turbulence model was used. It is a two equations model that convenient for moderate to high complexity flows [9]. The k-ε model solve two equation as follows [10]:
For turbulent kinetic energy k:

$$\frac{\partial(\rho k)}{\partial t} + \frac{\partial(\rho k u_i)}{\partial x_i} = \frac{\partial}{\partial x_j}\left[\frac{\mu_t}{\sigma_k}\frac{\partial k}{\partial x_j}\right] + 2\mu_t E_{ij}E_{ij} - \rho\varepsilon \quad (5)$$

For dissipation ε:

$$\frac{\partial(\rho\varepsilon)}{\partial t} + \frac{\partial(\rho\varepsilon u_i)}{\partial x_i} = \frac{\partial}{\partial x_j}\left[\frac{\mu_t}{\sigma_\varepsilon}\frac{\partial \varepsilon}{\partial x_j}\right] + C_{1\varepsilon}\frac{\varepsilon}{k}2\mu_t E_{ij}E_{ij} - C_{2\varepsilon}\rho\frac{\varepsilon^2}{k} \quad (6)$$

Geometry of runner wheel was designed in BladeGen considering hub diameter 0.398 m, outer diameter 0.996 m, blade thickness 0.002 m and initial blade angle as 60^0. The generated turbine blade with blade control curve is shown in figure 1. Spiral volute with guide vane was generated in Solidworks taking the volute inlet diameter as 1.1 m, vane inlet diameter 1.6 m, vane outlet diameter 1.05 m, hub diameter 0.28 m and vane inlet curve radius as 0.025 m. The generated geometry of the volute with guide vane is illustrated in figure 2.

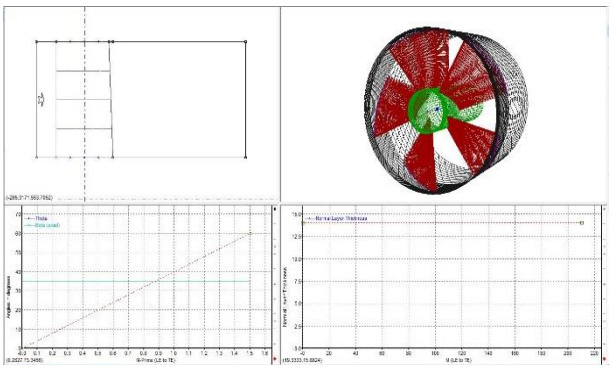

Fig. 1: Blade geometry with blade control curve.

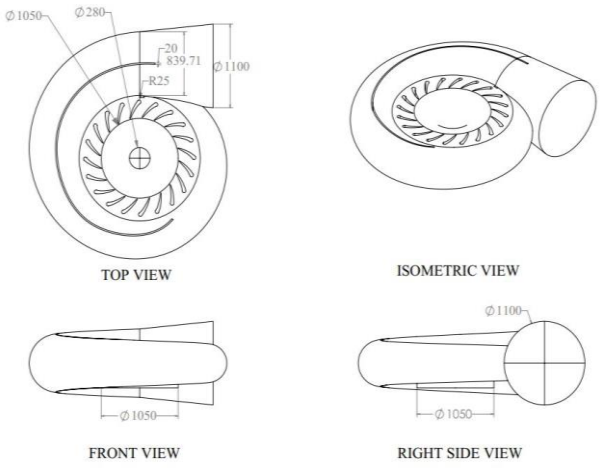

Fig. 2: Generated geometry of volute and guide vane.

Mesh of the turbine runner wheel, spiral volute with guide vane were generated in ANSYS Turbogrid as well as ANSYS mesh generator. Mesh were generated using patch conforming method and then inflation was done with respect to volute wall. First layer thickness was used as option of inflation, first layer height is 0.2 mm, maximum layer 15 and growth rate of 1.2 was used. Mesh of spiral volute contains 4522346 tetrahedral cells and the reason of using tetrahedral cell is it fits better with complex geometry. Figure 3 and figure 4 depict the generated mesh for turbine geometry.

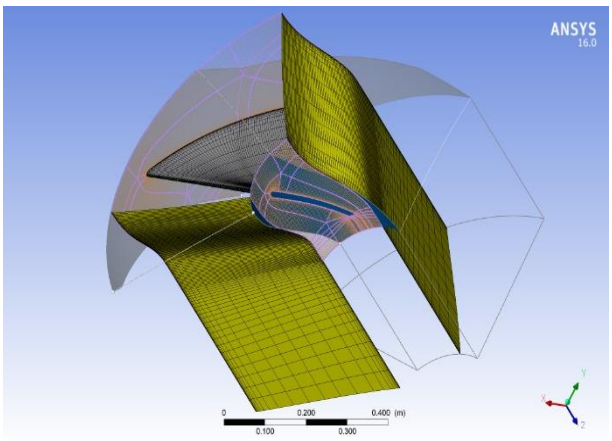

Fig. 3: Mesh generated for turbine blade.

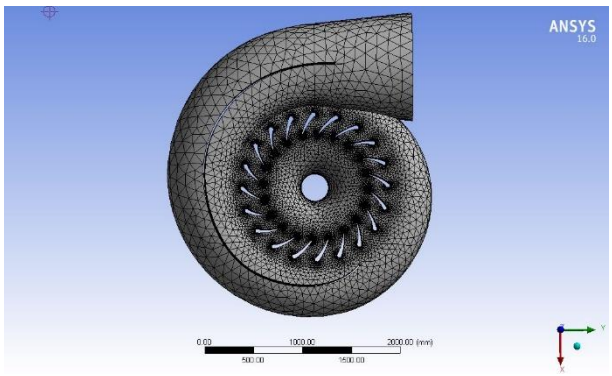

Fig. 4: Mesh generated for volute and guide vane.

3. Result and Discussion

Pressure and velocity changes of water in the turbine are observed and represented by figure 5 and figure 6. In the figure 5, a sharp decrease of water pressure can be seen from turbine inlet to outlet. The pressure falls to 19734.16 pa from 70898.85 pa and then there is a slight rise of pressure at 0.43 m from the inlet, then falls again to 20166.90 pa at 0.78 m. A gradual declination of the flow velocity can be observed in figure 6. The velocity

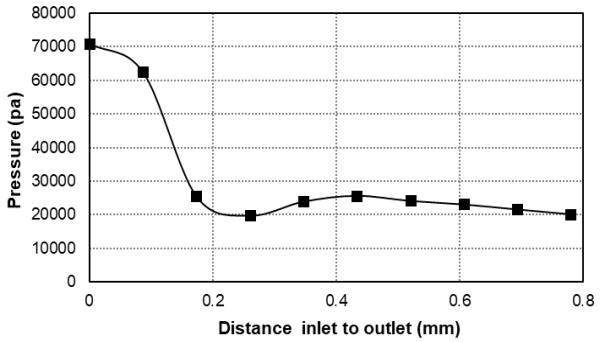

Fig. 5: Variation of pressure with distance.

decreases from 16.64 m/s to 8.43 m/s up to 0.43 m from the inlet and then velocity becomes constant. The degradation of flow velocity and pressure is due to the conversion of energy to produce power that rotate the turbine blade.

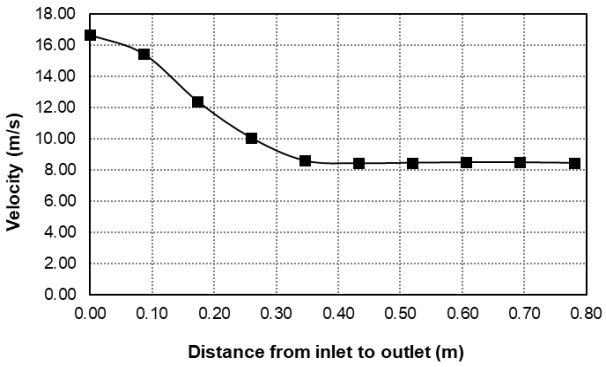

Fig. 6: Variation of flow velocity with distance.

The effect of load variations exerted on the rotating parts due to the pressure fluctuations can be observed through figure 7. Due to the varying loads on the stationary and rotating parts of the turbine, they suffer a lot as they are not designed for such operating conditions.

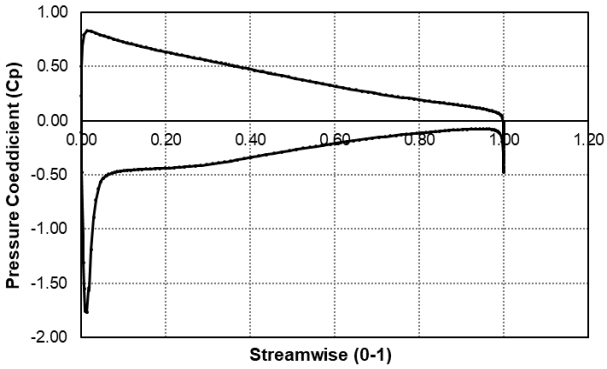

Fig. 7: Variation of streamwise blade loading.

Figure 8 to figure 11 show different contour of pressure distribution through the turbine volute and runner. The inlet pressure distribution can be observed by figure 8 in which the pressure diminishes radially and the

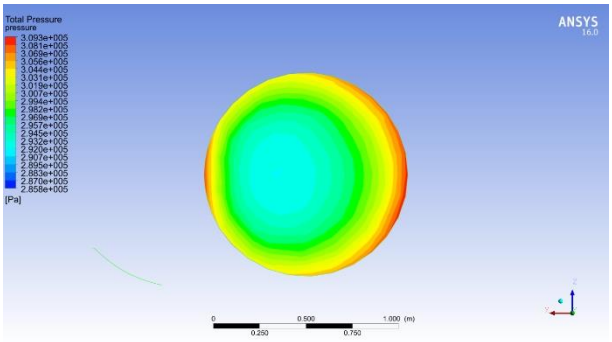

Fig. 8: Water pressure at inlet in last timestep.

the pressure near the wall is very higher than the center. Pressure distribution across turbine volute with guide vane and rotor blade is illustrated by figure 9. The pressure at volute inlet is very high and then there is a gradual loss of pressure. It can be seen that pressure above the blade is nearly 185 kpa and pressure is very low below the rotor blade. There is a pressure gradient across the rotor blade which is the main reason of creating the lift force responsible for the rotation of turbine blade.

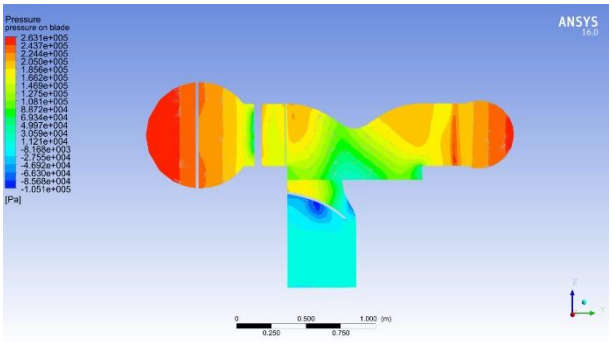

Fig. 9: Pressure distribution across turbine volute.

The pressure distribution along the rotor blade can be seen more clearly in figure 10 and figure 11. Pressure is much higher near the blade hub than the shroud. The lower portion experiences much lower fluid pressure than the upper portion.

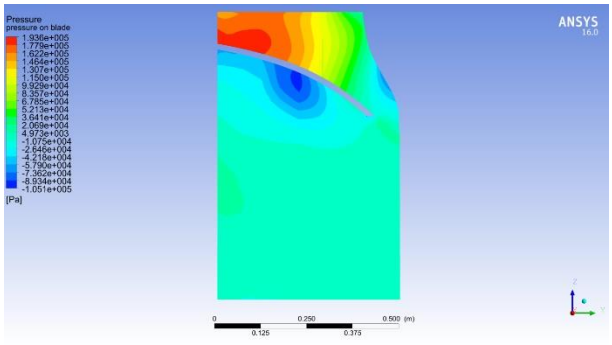

Fig. 10: Pressure distribution across blade.

The velocity distribution and velocity streamline contour are shown in figure 12 and figure 13. A slight increase in velocity is occurred in the lower portion of the

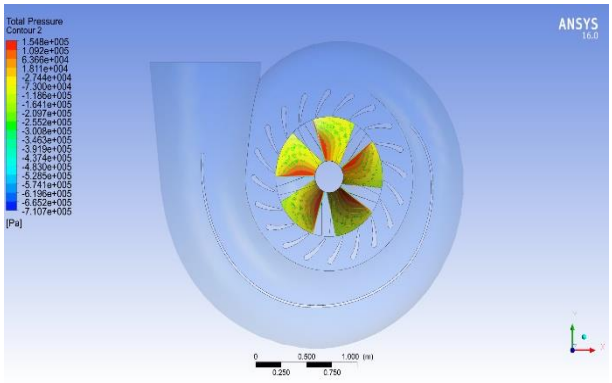

Fig. 11: Pressure distribution across blade.

blade. Figure 13 illustrates the velocity distribution across the volute and rotor blade more clearly. For the turbine runner wheel, the velocity drops from inlet to outlet. Near the casing, the changes of velocity are less as compared to the middle section. We can observe the variations of velocity as well as pressure for different parts of the Kaplan turbine through the color contour.

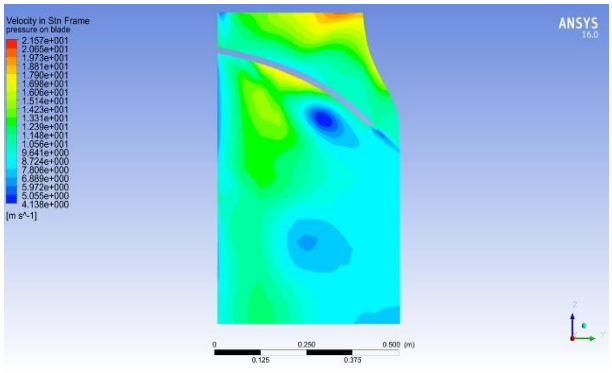

Fig. 12: Velocity distribution across rotor blade.

The velocity streamline in volute, turbine runner and draft tube region with the given geometry is shown in figure 14. From the turbine runner, the water flows with high velocity towards the draft tube. It can be seen by the green colored streamline near the draft tube section. This velocity head is transformed to pressure head which help producing more power.

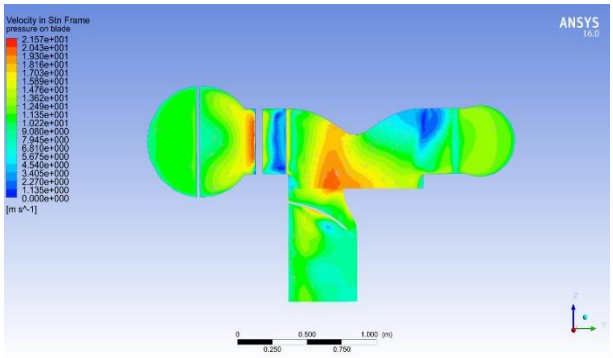

Fig. 13: Velocity distribution across volute.

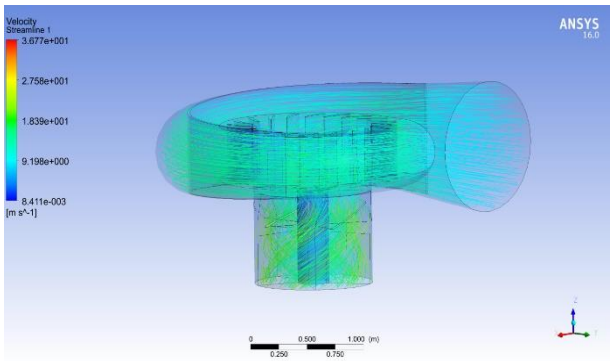

Fig. 14: Velocity streamline in turbine casing and rotor blade (front view).

4. Conclusion

In this research, the variation of pressure and velocity were observed for a certain amount of head and volume flow rate of water in Kaplan turbine. For that amount of head and flow rate, the pressure and velocity curves were graphically represented. The curves were obtained both for turbine runner wheel and the volute with guide vanes. Observed contours were attached with the paper for different parts, especially for the inlet, before the blades, after the blades as well as outlet. It is found that both the pressure and velocity reduce rapidly in the blade section which help to rotate the turbine blade. In this research work, only one shaped blades were used. Further simulations can be done with different types of blade shapes. In this paper, the number of blades as well as vane angle is also fixed. To analyze further on this topic, various number of blades can be introduced. Load on the turbine blade can be changed by changing the vane angle. To get optimized load of Kaplan turbine, we should do the simulation with various blade angle.

5. REFERENCES

[1] Munson, Bruce Roy, T. H. Okiishi, and Wade W. Huebsch. "Turbomachines." *Fundamentals of Fluid Mechanics*. 6th ed. Hoboken, NJ: J. Wiley & Sons, 2009.

[2] P. Celso, "Guide on How to Develop a Small Hydropower", *The European Small Hydropower Association*, Chapter 1, pp. 3-4, 2004.

[3] S.J.Williamson, B.H. Stark and J.D.Booker, "Low Head Pico Hydro Turbine Selection Using a Multi-Criteria Analysis", *World Renewable Energy Congress*, Volume 6, pp. 1377-1385, 2011.

[4] M.F. Jose, R.T. Erik, D.G. Oscar, and R.E. Reynaldo,"CFD Performance Evaluation and Runner Blades Design Optimization in a Francis Turbine", *ASME Conference Proceedings*, Volume 1, pp. 2253-2259, 2009.
[5] C. Abeykoon, T. Hantsch, “Design and analysis of a Kaplan turbine runner wheel.” *InProc. 3rd World Congr. Mech. Chem. Mater. Eng.* 2017. pp. 1-16.
[6] K. Amiri, B. Mulu, M. Raisee, MJ. Cervantes, “Unsteady pressure measurements on the runner of a Kaplan turbine during load acceptance and load rejection.” *Journal of Hydraulic Research*. Jan 2,2016. pp. 56-73.
[7] Charania, S. Shahil, V. Soni, C. Kiran, Patel, J. Desai, and V. Chauhan. "Evaluation of Vertical Kaplan Turbine using CFD." *Thirty Ninth National Conference on Fluid Mechanics and Fluid Power*, 2012.
[8] S. Muntean, RF Susan-Resiga, S. Bernad, A. Ioan. “Analysis of the GAMM Francis turbine distributor 3D flow for the operating range and optimization of the guide vane axis location.” *The 6th international conference hydrodynamics*, 2004. pp. 131-6.
[9] D. Jošt, A. Škerlavaj and A. Lipej, “Improvement of efficiency prediction for a Kaplan turbine with advanced turbulence models.” *Journal Mechanical Engineering*, *60*(2), 2014. pp.124-134.
[10] Motycak, Lukas, Ales Skotak, and Jiri Obrovsky, "Conditions of Kaplan turbine CFD analysis." *In ANSYS conference*, 2010.
[11] W. P. Jones and B. E. Launder, "The Prediction of Laminarization with a Two-Equation Model of Turbulence", *International Journal of Heat and Mass Transfer*, vol. 15, 1972. pp. 301-314.
[12] Versteeg, H. Kaarle; Malalasekera, Weeratunge, “An introduction to Computational Fluid Dynamics: The Finite Volume Method.” Pearson Education, 2007.

8. NOMENCLATURE

Symbol	Meaning	Unit
ρ	Density	(kg/m^3)
P	Pressure	(Pa)
u	Tangential velocity	(m/s)
D_a	Outer diameter	(m)
D_N	Hub diameter	(m)